Tetrahedron: *Asymmetry* 19 (2008) 2234–2239

Contents lists available at ScienceDirect

Tetrahedron: *Asymmetry*

journal homepage: www.elsevier.com/locate/tetasy

Asymmetric autocatalysis: crystallization-induced highly enantioselective synthesis of a conglomerating oxo-rhenium(V) complex

Witold K. Rybak *

Faculty of Chemistry, University of Wrocław, Joliot Curie 14, 50-383 Wrocław, Poland

ARTICLE INFO

Article history:
Received 11 July 2008
Accepted 19 September 2008
Available online 17 October 2008

ABSTRACT

Experiments designed to elucidate the mechanistic foundation and origins of enantioselectivity in a symmetry breaking synthesis are described. The autocatalytic enantioselective preparation of the title complex *cis*-[$ReOCl_2$(P ∼ O)py] [py = pyridine; P ∼ O = $(OCMe_2CMe_2O)POCMe_2CMe_2O^{(1-)}$], either *C* or *A* handed, from optically inactive substrates can be controlled by catalytic quantities of the non-racemic conglomerating product. The synthesis can be accomplished due to enantioselective complex formation and concomitant isomerization processes if the system reacts under strongly disturbed conditions (i.e., under vigorous stirring and boiling). For the first time we demonstrate practically that the two intrinsic mirror-image symmetry breaking phenomena, that is, enantioselective synthesis and spontaneous resolution of chemical compounds, can cooperate effectively leading to strong asymmetric amplification and high enantioselectivity in the system. When such cooperation is inadequate, sluggish deracemization occurs solely due to spontaneous resolution, known also as crystallization-induced asymmetric disequilibration mechanism. The experimental data obtained are in good accordance with recently developed theoretical models for chiral symmetry breaking processes. We assume that the system represents at least formally a highly efficient, inorganic, one-pot congener of the renowned organometallic Soai system.

1. Introduction

The origins of homochirality, a characteristic of living matter, have been an intellectually intriguing phenomenon for a long time.[1–3] Equally, the possible commercial applications of enantiomorphic substances and materials, taking advantage of their promising pharmaceutical, catalytic, magnetic, and non-linear optical properties, have provided a strong inspiration for materials-science and engineering research. Consequently, at least for the above reasons, processes that break mirror-image symmetry are reviewed with considerable frequency and such reviews are usually given much prominence.[1–10] There are currently two types of mirror-image symmetry breaking processes known in chemistry: 'spontaneous' asymmetric crystallization and 'spontaneous' asymmetric syntheses (by means of chemical reactions). Both involve the amplification of a tiny enantiomeric imbalance leading to the overwhelming enantioenrichment of acquiring substances either in the crystal state or in other states. However, there are only a few examples of well-documented spontaneous symmetry breaking crystallization, and even fewer of mirror-image symmetry breaking syntheses of chemical compounds.

Havinga was the first to recognize total spontaneous resolution of a conglomerate in the case of chiral ammonium salt, which was recently also explored by Kostyanovsky et al.[11,12] When *rac*-*N*,*N*,*N*,-allylethylmethylanilinium iodide is allowed to crystallize slowly from chloroform, it yields crystals in ample enantiomeric excess (*R* or *S*). A melt of chiral 1,1′-binaphthyl can crystallize as a racemate (mp 145 °C) or a conglomerate (mp 158 °C), frequently with one enantiomorph in excess randomly created when the melt is suddenly cooled[13] or stirred at 150 °C.[14] A supersaturated solution of easily interconverting complexes, $[(\text{L-ACL})_3NiCl_2]\leftrightarrow[(\text{D-ACL})_3NiCl_2]$ (ACL = α-amino-ε-caprolactam), is capable of preferential crystallization, depending on the handedness of the seeding crystal used.[15] Kondepudi et al. have shown that an exemplary and well-known conglomerate ($P2_13$) of achiral $NaClO_3$ can crystallize yielding almost exclusively left- or right-handed crystals from a supersaturated solution under strong stirring.[16] Furthermore, Håkansson et al. have even exploited stereochemically labile conglomerates for chirality transfer reactions in the solid state.[17] All of the above symmetry breaking crystallization processes strongly depend on prior seeding and provide a high enantiomeric excess (ee) of the products with seed-controlled preferential handedness. Those processes are feasible due to crystallization-induced asymmetric disequilibration of the racemate, also acknowledged as asymmetric transformation of the second kind.[18,19]

However, the most remarkable example of mirror-image symmetry breaking synthesis is the Soai system, that is, autocatalytic

* Tel.: +48 71 375 7355; fax: +48 71 375 7356.
E-mail addresses: rybak@wchuwr.pl, rybak@pop.e-wro.pl

0957-4166/$ - see front matter © 2008 Elsevier Ltd. All rights reserved.
doi:10.1016/j.tetasy.2008.09.019

alkylation of pyrimidyl aldehydes using ZnR_2 and involving the use of chiral product pyrimidyl alcohols as catalysts.[20–22] Such chirally autocatalytic syntheses have been studied under a variety of reaction conditions[23–25] and assessed by several other authors in order to rationalize their mechanism.[26–28] Asakura et al. have reported the generation of optically active *cis*-$[CoBr(NH_3)(en)_2]Br_2$ (en = 1,2-ethanediamine) from optically inactive substrates in a stirred suspension by a chiral autocatalysis mechanism.[29,30] However, more recently, Harris et al. have published results that weaken the case for the autocatalytic mechanism for the enantioselective formation of the above complex.[31] The complex *cis*-$[CoBr(NH_3)(en)_2]Br_2$ has been shown, by means of structure determination from powder X-ray diffraction data, to be a racemate rather than a conglomerate in the crystalline solid state. As conglomerate crystallization seems to be a prerequisite for spontaneous symmetry breaking, the results demonstrate, at least, that there is an intrinsic irreproducibility in this system. Gillard et al. have described the synthesis of the chiral polysulfide $(NH_4)_2$-$[Pt(S_5)(S_6)_2]\cdot 2H_2O$: the complex crystallizes spontaneously with one enantiomer in excess.[32] However, this system has not been explored in greater detail.

Over the last few years, active experimental studies based on a mechanistic approach to chiral symmetry breaking phase transitions, both solid–solution[33–35] and solid–gas,[36] have succeeded in significantly improving our understanding of the phenomena under consideration. While a stimulating scientific discussion on the fine details of the mechanism of symmetry breaking processes, both crystallization[37–41] and synthesis,[42–45] continues, theoretical reaction-type models have been developed that can describe the kinetics of the time evolution of a system toward homochirality.[46–49] Indeed, complete homochirality of products in a mirror-image symmetry breaking process (whether crystallization or synthesis) can be designed as a result of non-linear autocatalysis coupled with back-reaction recycling of achiral substrates in a closed system. Moreover, for an open-flow system (unlike in a closed system, the chiral products flow out from the reaction system), it has been shown that homochirality generation can be accomplished by a more general mechanism, even without a recycling reaction.[49] The applicability of these models to both processes (crystallization and synthesis) clearly suggests that under appropriate circumstances there may be an inherent mechanistic cooperation between these two phenomena (i.e., symmetry breaking crystallization and enantioselective chemical synthesis), as pointed out by Gridnev.[42] Very recently, Blackmond, Vlieg and their associates have reported the emergence of a single chiral solid state for an amino acid derivative starting from a nearly racemic mixture.[45]

Herein, we report the possibility of intrinsic cooperation between symmetry breaking chemical synthesis and crystallization. Such cooperation can be explicitly demonstrated for the case of enantioselective synthesis of the conglomerating title complex *cis*-$[ReOCl_2(P\sim O)py]$ [*cis*-**1**, py = pyridine; $P\sim O = (OCMe_2CMe_2O)$-$POCMe_2CMe_2O^{(1-)}$]. Appropriate adjustment of the kinetic-thermodynamic properties of this system allowed us to explore the mechanistic aspects of homochirality generation in the system. We report on some laboratory experiments demonstrating the intrinsic cooperation involved between the two symmetry breaking phenomena already at the stage of complex formation.

2. Results and discussion

During the course of our studies on the structural peculiarity of $ReOX_2(P\sim O)py$ diastereomers [X = Cl, Br, I; py = pyridine; $P\sim O = (OCMe_2CMe_2O)POCMe_2CMe_2O^{(1-)}$], we have been able to obtain the asymmetric, autocatalytic, and highly efficient preparation of one enantiomer (from optically inactive precursors) taking advantage of a subtle interplay between chiral conglomerating *cis* and achiral *trans*-oxo-rhenium diastereomeric complexes.[50–52] The *cis*- with *trans*-equilibrium reported in those papers is further discussed here in connection with three precursor reactions used to make the desired equilibrating rhenium complex. We focus on the synthesis, illustrated in Scheme 1, of chiral *cis*-$ReOCl_2(P\sim O)py$ *cis*-**1** as a conglomerate of *C*-$(+)_{589}$ and *A*-$(-)_{589}$ enantiomers,[†] which can be accomplished from optically inactive substrates in several ways. In a chelation reaction (1), achiral *trans*-$ReOCl_2(OEt)py_2$ and the optically inactive spirophosphorane $HP\sim O$ yield a racemic mixture of *cis*-**1** with the minor formation of *trans*-**1** owing to *cis*–*trans* equilibration (3), that is, isomerization reaction.[50,52] Secondly, *cis*-**1** can be obtained as a result of the substitution of pyridine for the monodentate ligand L in $ReOX_2(P\sim O)L$ (L = PPh_3, $OPPh_3$), (2).[‡] Finally, *cis*-**1** can be attained directly from *trans*-**1** through an intrinsic isomerization reaction (3). While reactions (1)–(3) proceed, the main product, chiral *cis*-**1**, precipitates from the toluene reaction mixture almost qualitatively, although the minor product, achiral *trans*-**1**, remains in solution (see Section 4). However, if these reactions are carried out in boiling toluene, under vigorous stirring conditions (1100 rpm) and in the presence of seeds of one enantiomer added in a small amount (1–2 mol %), they become either more or less enantioselective. The dependence of product accumulation and enantiomeric excess on the reaction time for syntheses (1) and (2) performed under the above conditions shows unexpectedly large dissimilarities (Fig. 1). While the chelation reaction (1) manifests a fairly slow buildup of *cis*-**1** with high enantiomeric excess (97.5%), the substitution of pyridine (2) is characterized by fast formation of *cis*-**1** with a rather low ultimate ee (4.2%).[§]

To rationalize this experimental peculiarity, one can tentatively postulate that different mechanisms operate in these two reactions. The different *trans*-**1** accumulation profiles for (1) and (2) (Fig. 1) may even suggest that reaction (1) proceeds with the prior formation of *trans*-**1** as an intermediate that then isomerizes to *cis*-**1**, while reaction (2) proceeds directly to chiral *cis*-**1**.

With a view to verifying this implication, the isomerization of *trans*-**1** to *cis*-**1** was put under scrutiny. The question that arises is what asymmetric amplification will occur if achiral *trans*-**1** is simply utilized as the substrate in the seeded synthesis of complex *cis*-**1** under similar reaction conditions. The dependence of formation yield and enantiomeric excess ee of *cis*-**1** on time in the seeded isomerization reaction (Fig. 2) shows, surprisingly, relatively slow asymmetric amplification followed by rapid formation of *cis*-**1**.

This sequence is opposite to that observed in the case of a seeded chelation reaction [(1) in Fig. 1], but is similar to reaction (2). While 95% ee (at ca. 50% yield) is reached in the reaction of (1) after 1 h [Fig. 1(1)], in the case of isomerization 95% ee requires more than 10 h (though with 90% yield of *cis*-**1**) if a suitable, ample quantity of the seeds (8 mol %) is applied (Fig. 2a). Besides, in contrast to reaction (1), the isomerization reaction (3) manifests a significant tendency for the asymmetric amplification profile to be influenced by the amount of seeds. At a small quantity of seeds (0.8 mol %), the system relatively quickly attains the level of ca. 35% ee, subsequently evolving slowly over more than ten days to higher enantiomeric enrichment (94.5% ee after 15 days, Fig. 2b).

These results clearly reveal that two coupled stages are operating in the system: the enantioselective formation of *cis*-**1** proceeds alongside the autocatalytic enantiomeric reinforcement, as shown

[†] *C* and *A* refer to clockwise and anti-clockwise arrangements of the ligands in a coordination polyhedron.

[‡] Although further discussion is narrowed to the complex where L = $OPPh_3$, very similar features were observed for a substrate with L = PPh_3.

[§] The values of both ee and the yield of *cis*-**1** are given after correction for the initially added product catalyst, see Section 4.

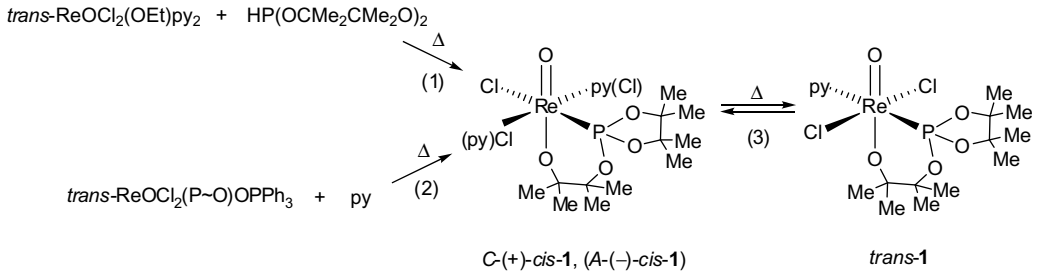

Scheme 1.

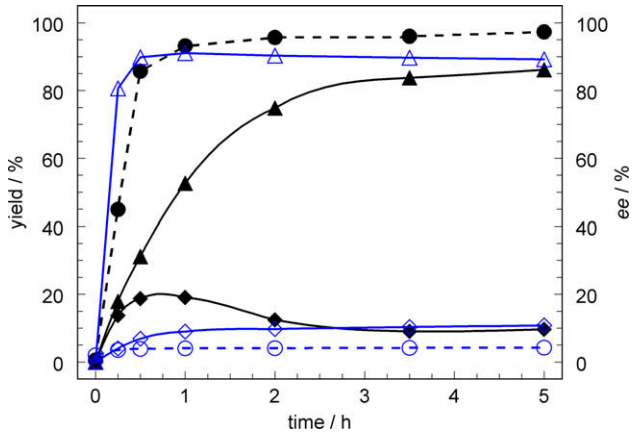

Figure 1. Time evolution of product accumulation (solid lines, left axis) of *cis*-**1** (triangles ▲, △) and *trans*-**1** (diamonds ♦, ◇) and enantiomeric excess (broken lines, right axis) of *cis*-**1** (circles ●, ○) in two asymmetric autocatalytic reactions shown in Scheme 1: (1) plotted with solid symbols, and (2) plotted with outline symbols. The syntheses were carried out in boiling toluene (12 mL), under vigorous stirring (1100 rpm), with initially added seeds (*C*-(+)-*cis*-**1**, 2 mol %, ee = +99.5%): *trans*-$ReOCl_2(OEt)py_2$ (0.225 mmol) and HP ~ O (0.65 mmol) in (1); *trans*-$ReOCl_2(P \sim O)OPPh_3$ (0.225 mmol) and py (0.35 mmol) in (2).

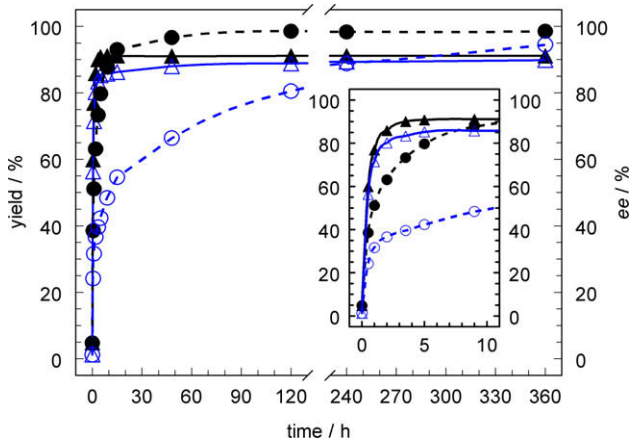

Figure 2. Reaction yield (triangles, solid lines, left axis) and enantiomeric excess (circles, broken lines, right axis) of *cis*-**1** vs time in the isomerization reaction (3) of *trans*-**1** (0.225 mmol) carried out in boiling toluene (12 mL), with vigorous stirring (1100 rpm) and seeds (*C*-(+)-*cis*-**1**, ee = +99.5%) initially added: (a) in 8 mol %, plotted with solid symbols (▲, ●); (b) in 0.8 mol %, plotted with outline symbols △, ○.

in Scheme 2. The enantiomeric reinforcement is sustained owing to autocatalytic seeded crystallization triggered by the crushed seed crystals (as a result of vigorous stirring), sparsely dissolved in the reaction mixture. Thus, enantiomorph crystal growth proceeds by incorporating homochiral molecules from the solution, thus

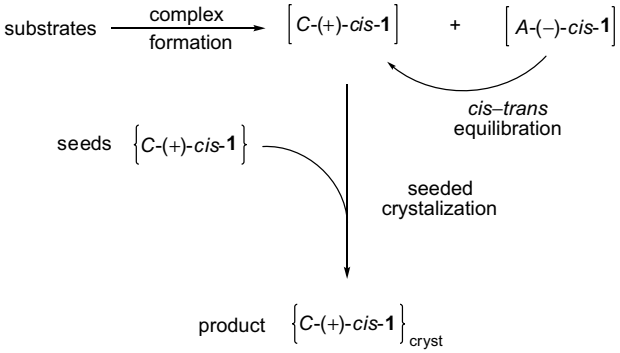

Scheme 2.

depleting the solution of solute molecules of the same handedness. This enantiomer depletion is reversed by the enantioselective formation of *cis*-**1** both as a result of synthesis (1, 2), and by *cis–trans* equilibration (3), although with supposedly different rates and contributions. Ultimately, these three cooperating processes: complex formation, autocatalytic seeded crystallization, and *cis–trans* equilibration become enantioselective and drive the system toward complete homochiral purity (Scheme 2). In fact, this *cis–trans* equilibration reaction plays the role of a racemization process that recycles two competitive enantiomers, relatively stable in solution, and provides back-reaction recycling of the achiral substrate *trans*-**1**.

Moreover, the results obtained show that the prior formation of *trans*-**1** as an intermediate does not seem to be a prerequisite for effective asymmetric amplification observed in the seeded chelation reaction (1). Instead, the rate of the *cis*-**1** ($\{C$-(+)-*cis*-$\mathbf{1}\}_{cryst}$) conglomerate crystal deposition in Scheme 2 and the rates of *cis*-**1** complex formation are essential to accomplish and control asymmetric amplification in the system. However, if the *cis–trans* equilibration reaction is the only source of *cis*-**1** supply and this equilibration is relatively sluggish with respect to conglomerate crystal deposition, the autocatalytic enantiomeric reinforcement and deracemization become very slow and take weeks instead of hours. Figure 3 shows the enantiomeric excess as a function of time for the autocatalytic complete deracemization of two non-racemic samples of *cis*-**1** (with different initial ee of (+) or (−) handedness) carried out at similar reaction conditions as in Figure 2.

The rate profile of enantiomeric enhancement shows an autocatalytic appearance (S-shaped upper curve with the characteristic induction period), and the maximum rate is attained after a prolonged reaction time (ca. 9 days). The lower profile shows the deracemization rate for the sample prepared from the pure enantiomers starting with initial enrichment close to the level attained by the upper sample after about 9 days. Hence, no induction period can be observed for the complete deracemization in this case. These results clearly demonstrate that a sluggish spontaneous resolution mechanism operates in this system with a considerable

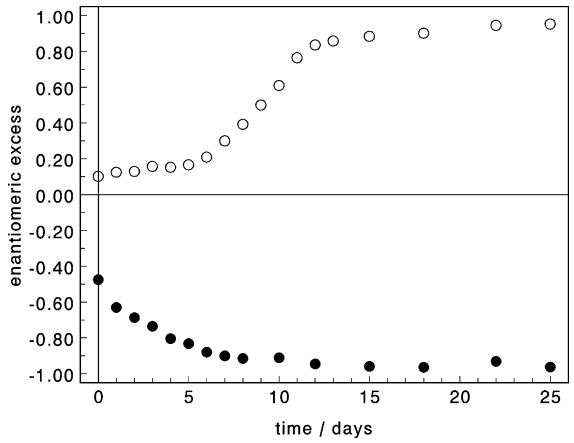

Figure 3. Time evolution of enantiomeric excess for two non-racemic samples of *cis*-**1**, either (+) or (−) handed, under prolonged stirring (1100 rpm) and in boiling toluene (12 mL). The upper part, plotted with outline circles (○), represents a sample composed of *rac*-*cis*-**1** (0.13771 g, 0.2237 mmol) and *C*-(+)-*cis*-**1** (0.01573 g, 0.02555 mmol) with ee = +0.102. The lower part, plotted with solid circles (●), represents a sample prepared from *A*-(−)-*cis*-**1** (0.1097 g, 0.1782 mmol) and *C*-(+)-*cis*-**1** (0.03903 g, 0.0634 mmol) with ee = −0.475. Periodically small solid samples of the reaction mixture (⩾0.002 g) were collected by filtration with the aim of measuring optical rotation and assessing enantiomeric excess (ee).

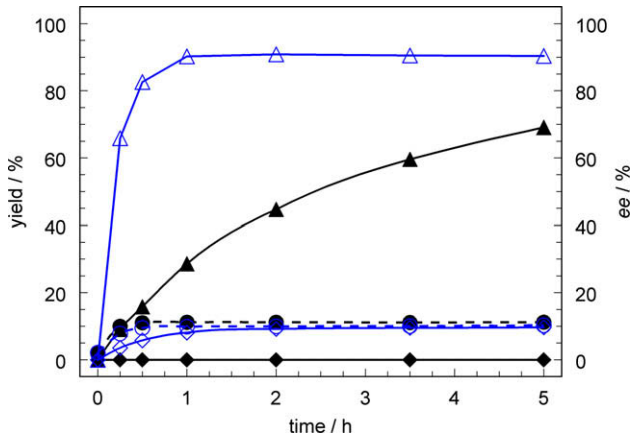

Figure 4. Time evolution of product accumulation (solid lines, left axis) of *cis*-**1** (triangles ▲, △) and *trans*-1 (diamonds ♦, ◇) and enantiomeric excess (broken lines, right axis) of *cis*-**1** (circles ●, ○) in the two asymmetric autocatalytic reactions shown in Scheme 1: (1) plotted with solid symbols, and (2) plotted with outline symbols. The syntheses were carried out with vigorous stirring (1100 rpm), and initially added seeds (*C*-(+)-*cis*-1, 2 mol %, ee = +99.5%): *trans*-$ReOCl_2(OEt)py_2$ (0.225 mmol) and HP∼O (0.65 mmol) in boiling *n*-octane (12 mL) in (1); *trans*-$ReOCl_2(P{\sim}O)OPPh_3$ (0.225 mmol), $OPPh_3$ (2.25 mmol) and py (0.35 mmol) in boiling toluene (12 mL) in (2).

dependence on the initial abundance of enantiomers in the reaction mixture. For a stirred slurry of *rac*-*cis*-**1** in the absence of enantiomeric seeds, the solid ee remained unchanged over the same period.

Furthermore, if the rate of *cis*-**1** formation in the chemical synthesis and both of the above controlling rates (i.e., conglomerate crystallization–dissolution and *cis*–*trans* equilibration) are comparable, the seeds that trigger the conglomerate formation can drive enantioselective complex formation and facilitate amplification to a significant extent, as in the case of the seeded chelation reaction ((1), Fig. 1). In contrast, if the *cis*-**1** formation reaction is too fast relative to the above controlling rates, the asymmetric amplification is rather poor (the rates of conglomerate crystallization–dissolution and *cis*–*trans* equilibration remain much the same for all three of the examined reactions (1)–(3) at similar reaction conditions). The latter case is exemplified by the pyridine substitution seeded reaction [(2), Fig. 1]. Afterwards, the poorly enriched system very slowly attains complete enantiomeric enrichment solely due to spontaneous resolution processes involving conglomerate crystallization and *cis*–*trans* equilibration, which are also acknowledged as crystallization-induced asymmetric disequilibration (shown in Figs. 2b and 3).

Incidentally, these observations are in good agreement with the consequences of the theoretical model of Saito and Hyuga for autocatalytic asymmetric chemical reactions in open-flow systems, which clearly explain the mechanism of homochirality selection by the system, either with or without the involvement of inherent recycling processes.[49] We suppose that in our system, an open-flow model is realized by the slow chelation reaction (1) as the influx of the substrate and conglomerate crystallization as the efflux of the chiral product.

In order to corroborate this proposition, the seeded synthesis (1) was carried out under similar conditions as in Figure 1(1), except for the use of *n*-octane as the solvent instead of toluene ((1) in Fig. 4). A much poorer solvent for all reactants and in particular for *cis*-**1**, octane makes possible the fairly slow formation of the complex *cis*-**1** and prevents *cis*–*trans* equilibration recycling substantially if not completely. However, it should be noted that the seed-originated catalyst *C*-(+)-*cis*-**1**, because of its lower solubility, will operate in the octane reaction solution at a much lower concentration than in toluene. As a result, after half an hour's reaction time the system attains ca. 11% enantiomeric excess, which remains quite stable with no detectable formation of *trans*-**1**, but with slow accumulation of *cis*-**1**, reaching 69% yield after five hours.

Finally, in order to evaluate the mechanism under discussion we performed another seeded reaction (2) under the same conditions as in Figure 1(2), except for the addition of $OPPh_3$ in 10-fold molar excess (2.25 mmol), so as to slow down the pyridine substitution reaction and *cis*-**1** formation ((2) in Fig. 4). In addition, this retardation may relatively promote the contribution of the *cis*–*trans* recycling of the enantiomers and eventual conglomerate formation, making the synthesis more enantioselective. Indeed, the seeded synthesis (2) under the above conditions over the same reaction time (5 h) gives a more-than-twice-higher enantiomeric excess (10.3% currently vs 4.2% formerly) at a similar reaction yield (90.3% vs 88.9%, respectively).

In our opinion, all these experimental facts firmly support the mechanism depicted in Scheme 3, which couples the synthesis and crystallization symmetry breaking processes. If this heterogeneous (solid/solution) reacting system is not perturbed (e.g., by vigorous boiling, stirring, and seeding), it degenerates, yielding a generally racemic mixture of the asymmetric synthesis product. However, if the system reacts under strongly disturbed conditions, yet without seeding, it evolves to a bifurcated bimodal one, with a random distribution of the enantiomers.[50] Finally, additional seeding and physical perturbations cause the system to undergo an autocatalytic symmetry breaking process at the same reaction time, yielding a product with one enantiomer in excess, with the same handedness as the seeds. To rationalize this autocatalytic process, one can point to the prerequisite initial aggregation in solution of several homochiral molecules as a transient but crucial step in the homochiral crystal growing process. This aggregation can be effectively catalyzed by homochiral molecules originated from the sparsely dissolving crystals of the product seeds. These product-molecule-containing aggregates can easily clusterize toward the formation of primary crystal nuclei or assemble with secondary nuclei created from crushed seeds and ultimately form an enantiomorph crystalline product accomplishing the autocatalytic cycle.

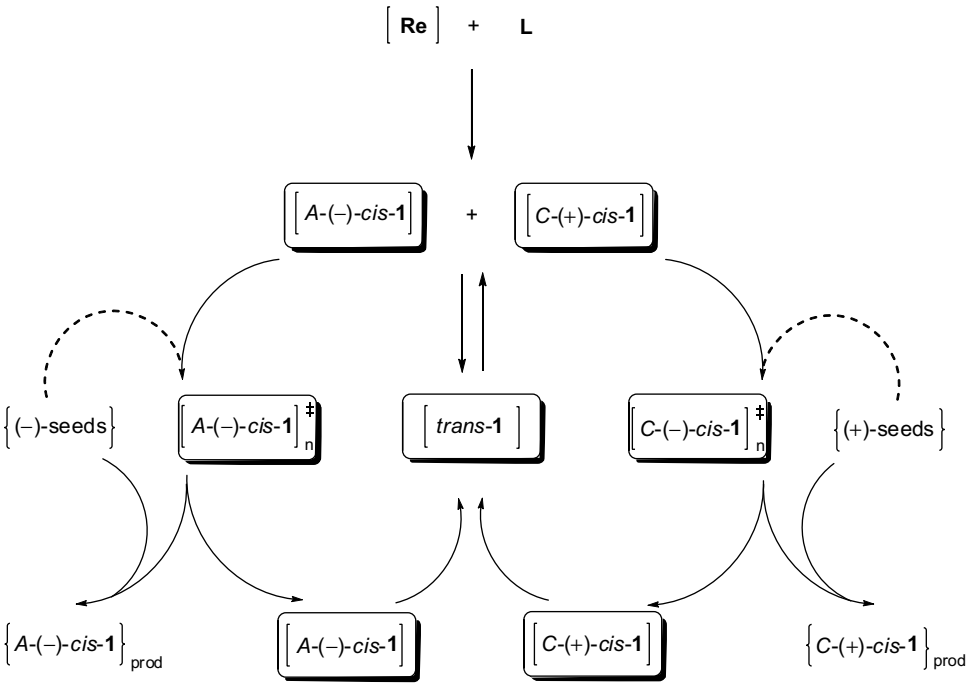

Scheme 3. [Re] and L symbolize the substrates (see Scheme 1). Liquid-phase species are indicated by square brackets while solids are shown in braces. The transient homochiral aggregate, the supposedly conglomerating crystallite precursors are labeled with the not-equal-to sign ≠. Dashed arrows represent the sparse dissolution of the seed crystals.

3. Conclusion

It should be noted that the efficiency of the mirror-image symmetry breaking synthesis strongly depends on the inherent kinetics and the subtle interplay of the complex controlling heterogeneous processes, and in particular the aggregation, primary and secondary nucleation, crystallite conglomerate formation–dissolution, and racemization steps.[40,41] However, these complex controlling heterogeneous processes can be successfully coupled to the synthesis of the conglomerating compound that proceeds at the same time. When these coupled processes happen to be appropriately tuned, the system can promote homochirality with high efficiency.

The results obtained show that by modifying the experimental reaction conditions it is possible to control the outcome of the synthesis. Occasionally, under favorable confinement conditions the two-stage coupled mechanism (i.e., enantioselective synthesis of a chemical compound and its conglomerate formation) provides a really high asymmetric amplification.

Consequently, such behavior is promising for managing and exploiting this phenomenon in other conglomerating and stereochemically fluxional systems, which appear not to be very rare in transition metal coordination chemistry.[53] Moreover, the results obtained allow us to present new, more general, mechanistic insights into the autocatalytic asymmetric synthesis of chemical compounds that can be triggered by conglomerating crystallization. These observations may also have considerable implications for new procedures development in valuable chemicals or materials-processing contexts. Ongoing studies include expanding the scope and utility of these observations. Finally, we can presume that our system may represent an inorganic one-pot congener of the renowned organometallic Soai system, at least formally, especially as the involvement of higher-order aggregates and product precipitation has been detected in the latter system.[28]

4. Experimental

4.1. General

All preparations were performed under dry, oxygen-free nitrogen. Toluene and *n*-octane were thoroughly dried by standard procedures and distilled prior to use. Other solvents and reagents obtained from commercial sources were used without further purification. ^{1}H and ^{31}P NMR spectra were recorded with a Bruker AMX (300 MHz for ^{1}H NMR). The chemical shifts (δ) are given in ppm toward TMS (^{1}H) and H_3PO_4 (^{31}P) using CD_2Cl_2 solvent as lock and reference (^{1}H). The optical rotation α_{589} was measured for CH_2Cl_2 solutions in a 5 cm cell at 20 °C with a Jasco DIP 1000 polarimeter. The ligands $HP(OCMe_2CMe_2O)_2$,[54] *cis*-$ReOCl_2(P\sim O)py$[54] *cis*-**1**, and *trans*-$ReOCl_2(P\sim O)L$, (L = py,[52] PPh_3,[54] $OPPh_3$[54]) were prepared according to literature procedures.

4.2. General procedure used for the study of symmetry breaking autocatalytic reactions (1) and (2) and *trans–cis* isomerization (3) (Scheme 1)

The substrates relevant to reaction (1) (*trans*-$ReOCl_2(OEt)py_2$ (0.225 mmol) and $HP(OCMe_2CMe_2O)_2$ (0.65 mmol, $HP\sim O$)), reaction (2) (*trans*-$ReOCl_2(P\sim O)OPPh_3$ (0.225 mmol), py (0.35 mmol), and if applicable $OPPh_3$ (2.25 mmol)), or reaction (3) (*trans*-$ReOCl_2(P\sim O)py$ (0.225 mmol, *trans*-**1**), with the addition of appropriate amounts of finely ground seeds (0.5–10% mol Re/mol Re, ee = +99.5%)) were placed with dried solvents, either toluene or *n*-octane (12 mL), in a 50 mL Schlenk flask under nitrogen. The flask, equipped with an octagonal Teflon® stir-bar (16 × 7 mm), a condenser, and an oil bubbler, was placed in an oil bath heated to 125 °C. The reaction mixture was boiled and powerfully stirred (ca. 1100 rpm, with IKA® RET digi-visc) for either 5 h or a longer time. These preparations afford the almost insoluble *cis*-**1** (⩽0.005 g *rac*-*cis*-**1** per 100 mL of toluene at 110 °C) and the readily

soluble *trans*-**1** (3 g per 100 mL of toluene at 20 °C) as the only rhenium products. To follow the reaction progress, several small samples (0.2 mL) of the reaction mixture were collected periodically as a suspension in NMR tubes. Volatiles were evaporated to dryness (by means of freeze–thaw cycles under vacuum), and the residue was weighed and dissolved in CD_2Cl_2 in order to record the NMR spectra and evaluate the composition of the sample. Finally, the sample was diluted with CH_2Cl_2 in a volumetric flask (5 mL) to measure optical rotation and to assess enantiomeric excess (ee). The specific rotation was $[a]_{589} = +1380$ (c 0.05 g per 100 mL in CH_2Cl_2) for the pure enantiomer *C*-(+)-*cis*-**1**. The results were averaged from experiments repeated twice. To evaluate intrinsic asymmetric amplification, the 'reduced' ee values of the product (ee_{cor}), after deduction of the effect of the initial catalyst on the ee values of the obtained product *cis*-**1**, were calculated: $ee_{cor} = (ee_1 - (n_0 \times ee_0/n_1)) \times (n_1/(n_1 - n_0))$, where ee_1 is the observed ee value of the obtained product, ee_0 is the ee value of the initially added catalyst, n_0 is the catalyst initially added contained in the sample [mmol], and n_1 is the total obtained *cis*-**1** product in the sample [mmol]. Occasionally, the CD spectra of the samples were recorded in order to check the correct assessment of enantiomeric excess estimated through optical rotation measurements.

Acknowledgment

Financial support with Grant PBZ-KBN-118/T09/2007 is gratefully acknowledged.

References

1. Cintas, P. *Angew. Chem., Int. Ed.* **2002**, *41*, 1139–1145 and references cited therein.
2. Mislow, K. *Collect. Czech. Chem. Commun.* **2003**, *68*, 849–864 and references cited therein.
3. Weissbuch, I.; Leiserowitz, L.; Lahav, M. *Top. Curr. Chem.* **2005**, *259*, 123–165 and references cited therein.
4. Avalos, M.; Babiano, R.; Cintas, P.; Jimenez, J. L.; Palacios, J. C. *Chem. Commun.* **2000**, 887–892.
5. Soai, K.; Shibata, T.; Sato, I. *Acc. Chem. Res.* **2000**, *33*, 382–390.
6. Kondepudi, D. K.; Asakura, K. *Acc. Chem. Res.* **2001**, *34*, 946–954.
7. Todd, M. H. *Chem. Soc. Rev.* **2002**, *31*, 211–222.
8. Mikami, K.; Yamanaka, M. *Chem. Rev.* **2003**, *103*, 3369–3400.
9. Blackmond, D. G. *Proc. Natl. Acad. Sci. U.S.A.* **2004**, *101*, 5732–5736.
10. Kostyanovsky, V. R. *Mendeleev Commun.* **2003**, 85–90.
11. Havinga, E. *Biochim. Biophys. Acta* **1954**, *13*, 171.
12. Kostyanovsky, R. G.; Kostyanovsky, V. R.; Kadorkina, G. K.; Lyssenko, K. A. *Mendeleev Commun.* **2001**, 1–5.
13. Wilson, K. R.; Pincock, R. E. *J. Am. Chem. Soc.* **1975**, *97*, 1474–1478.
14. Kondepudi, D. K.; Laudadio, J.; Asakura, K. *J. Am. Chem. Soc.* **1999**, *121*, 1448–1451.
15. Sifiniades, S.; Boyle, W. J.; Van Peppen, J. F., Jr. *J. Am. Chem. Soc.* **1976**, *98*, 3738–3739.
16. Kondepudi, D. K.; Bullock, K. L.; Digits, J. A.; Hall, J. K.; Miller, J. M. *J. Am. Chem. Soc.* **1993**, *115*, 10211–10216.
17. Johansson, A.; Håkansson, M. . *Chem.-Eur. J* **2005**, *11*, 5238–5248.
18. Jacques, J.; Collet, A.; Wilen, S. H. *Enantiomers*; W. Krieger: Malabar, FL, USA, 1994. pp 369–371.
19. Eliel, E. L.; Wilen, S. H.; Mander, L. N. *Stereochemistry of Organic Compounds*; Wiley: New York, 1994. pp 315–322.
20. Soai, K.; Shibata, T.; Morioka, H.; Choji, K. *Nature* **1995**, *378*, 767–768.
21. Sato, I.; Urabe, H.; Ishiguro, S.; Shibata, T.; Soai, K. *Angew. Chem., Int. Ed.* **2003**, *42*, 315–317.
22. Soai, K.; Kawasaki, T. *Chirality* **2006**, *18*, 469–478.
23. Soai, K.; Sato, I.; Shibata, T.; Komiya, S.; Hayashi, M.; Matsueda, Y.; Imamura, H.; Hayase, T.; Morioka, H.; Tabira, H.; Yamamotoa, J.; Kowata, Y. *Tetrahedron: Asymmetry* **2003**, *14*, 185–188.
24. Sato, I.; Kadowaki, K.; Ohgo, Y.; Soai, K. *J. Mol. Catal. A: Chem.* **2004**, *216*, 209–214.
25. Kawasaki, T.; Suzuki, K.; Licandro, E.; Bossi, A.; Maiorana, S.; Soai, K. *Tetrahedron: Asymmetry* **2006**, *17*, 2050–2053.
26. Singleton, D. A.; Vo, L. K. *Org. Lett.* **2003**, *5*, 4337–4339.
27. Gridnev, I. D.; Brown, J. M. *Proc. Natl. Acad. Sci. U.S.A.* **2004**, *101*, 5727–5731.
28. Buono, F. G.; Iwamura, H.; Blackmond, D. G. *Angew. Chem., Int. Ed.* **2004**, *43*, 2099–2103.
29. Asakura, K.; Kobayshi, K.; Mizusawa, Y.; Ozawa, T.; Osanai, S.; Yoshikawa, S. *Phys. D* **1995**, *84*, 72–78.
30. Asakura, K.; Ikumo, A.; Kurihara, K.; Osanai, S.; Kondepudi, D. K. *J. Phys. Chem.* **2000**, *104*, 2689–2694.
31. Guo, F.; Casadesus, M.; Cheung, E. Y.; Coogan, M. P.; Harris, K. D. M. *Chem. Commun.* **2006**, 1854–1856.
32. Evans, E. H. M.; Richards, J. P. G.; Gillard, R. D.; Wimmer, F. L. *Nouv. J. Chim.* **1986**, *10*, 783–791.
33. Viedma, C. *Phys. Rev. Lett.* **2005**, *94*. 065504(1–4).
34. Viedma, C. *Astrobiology* **2007**, *7*, 312–319.
35. Klussmann, M.; Izumi, T.; White, A. J. P.; Armstrong, A.; Blackmond, D. G. *J. Am. Chem. Soc.* **2007**, *129*, 7657–7660.
36. Fletcher, S. P.; Jagt, R. B. C.; Feringa, B. *Chem. Commun.* **2007**, 2578–2580.
37. Crusats, J.; Veintemillas-Verdaguer, S.; Ribo, J. M. *Chem.-Eur. J* **2007**, *13*, 10303–10305.
38. Blackmond, D. G. *Chem.-Eur. J* **2007**, *13*, 10306–10311.
39. Blackmond, D. G.; Klussmann, M. *Chem. Commun.* **2007**, 2578–2580.
40. Kondepudi, D. K.; Crook, K. E. *Cryst. Growth Des.* **2005**, *5*, 2173–2179.
41. Cartwright, J. H. E.; Piro, O.; Tuval, I. *Phys. Rev. Lett.* **2007**, *98*, 5501.
42. Gridnev, I. D. *Chem. Lett.* **2006**, *35*, 148–153.
43. Blackmond, D. G. *Tetrahedron: Asymmetry* **2006**, *17*, 584–589.
44. Klussmann, M.; Iwamura, H.; Mathew, S. P.; Wells, D. H., Jr.; Pandya1, U.; Armstrong, A.; Blackmond, D. G. *Nature* **2006**, *441*, 621–623.
45. Noorduin, W. L.; Izumi, T.; Millemaggi, A.; Leeman, M.; Meekes, H.; Van Enckevort, W. J. P.; Kellogg, R. M.; Kaptein, B.; Vlieg, E.; Blackmond, D. G. *J. Am. Chem. Soc.* **2008**, *130*, 1158–1159.
46. Saito, Y.; Hyuga, H. *J. Phys. Soc. Jpn.* **2004**, *73*, 33–35.
47. Uwaha, M. *J. Phys. Soc. Jpn.* **2004**, *73*, 2601–2603.
48. Saito, Y.; Hyuga, H. *J. Phys. Soc. Jpn.* **2005**, *74*, 535–537.
49. Saito, Y.; Hyuga, H. *J. Phys. Soc. Jpn.* **2005**, *74*, 1629–1635.
50. Rybak, W. K.; Skarżyńska, A.; Głowiak, T. *Angew. Chem., Int. Ed.* **2003**, *42*, 1725–1727.
51. Rybak, W. K.; Skarżyńska, A. *New J. Chem.* **2003**, *27*, 1687–1689.
52. Rybak, W. K.; Skarżyńska, A.; Szterenberg, L.; Ciunik, Z.; Głowiak, T. *Eur. J. Inorg. Chem.* **2005**, 4964–4975.
53. See for instance, the series of papers by I. Bernal on 'the phenomenon of conglomerate crystallization', for example Saha, M. K.; Ramanujam, R.; Bernal, I.; Fronczek, F. R. *Cryst. Growth Des.* **2002**, *2*, 205–212. and references cited therein.
54. Głowiak, T.; Rybak, W. K.; Skarżyńska, A. *Polyhedron* **2000**, *19*, 2667–2672.